Title

Allometric scaling of estuarine ecosystem metabolism

Journal

Proceedings of the National Academy of Sciences of the United States of America, 115(26)

ISSN

0027-8424

Author

Nidzieko, Nicholas J

Publication Date

2018-06-26

DOI

10.1073/pnas.1719963115

Peer reviewed

Allometric scaling of estuarine ecosystem metabolism

Nicholas J. Nidzieko[a,1]

[a]Department of Geography, University of California, Santa Barbara, CA 93106

Edited by Jonathan J. Cole, Cary Institute of Ecosystem Studies, Avon, NC, and approved May 14, 2018 (received for review November 21, 2017)

There are still significant uncertainties in the magnitude and direction of carbon fluxes through coastal ecosystems. An important component of these biogeochemical budgets is ecosystem metabolism, the net result of organismal metabolic processes within an ecosystem. In this paper, I present a synthesis of published ecosystem metabolism studies from coastal ecosystems and describe an empirical observation that size-dependent patterns in aquatic gross primary production and community respiration exist across a wide range of coastal geomorphologies. Ecosystem metabolism scales to the 3/4 power with volume in deeper estuaries dominated by pelagic primary production and nearly linearly with area in shallow estuaries dominated by benthic primary production. These results can be explained by applying scaling arguments for efficient, directed transport networks developed to explain similar size-dependent patterns in organismal metabolism. The main conclusion from this synthesis is that the residence time of new, nutrient-rich water is a fundamental organizing principle for the observed patterns. Residence time changes allometrically with size in pelagic ecosystems because velocities change by only an order of magnitude across systems that span more than ten orders of magnitude in size. This nonisometric change in velocity with size requires lower specific metabolic rates at larger ecosystem sizes. This change in transport may also explain a shift from predominantly net heterotrophy to net autotrophy with increasing size. The scaling results are applied to the total estuarine area in the continental United States to estimate the contribution of estuarine systems to the overall coastal budget of organic carbon.

ecosystem metabolism | estuaries | primary production | allometric scaling | metabolic theory

Coastal margins are home to some of the most productive habitats on the planet (1, 2), yet there is still a great deal of uncertainty about the sources, exchanges, and fates of carbon and nitrogen at the land/ocean interface (3). Scaling up in situ measurements to estimates of how these habitats contribute to global biogeochemical cycling (4, 5) has been hindered by their apparent heterogeneity, complex circulation, diverse geomorphology, and sizes that range from tens of meters to hundreds of kilometers. Consequently, processes that occur in coastal margin habitats are poorly represented in global models (6) despite the fact that these habitats are sites where terrestrial materials undergo significant transformations en route to the global oceans (7) and provide critical human ecosystem services (8).

Ecosystem metabolism refers to the collective formation and utilization of organic matter within an ecosystem (9). Since the seminal work of H. T. Odum (10), the concept has more than tacitly drawn a parallel between estuaries and living organisms: "Each day as the sun rises and retires the beautiful green bays like great creatures breathe in and out" (ref. 11, p. 16). Just as organismal metabolism is the sum of cellular metabolic rates, the "composite metabolism" (11) of an ecosystem is the sum of the metabolic processes of its constituent organisms. The difference in gross primary production (in which photosynthetic autotrophs fix inorganic carbon into organic forms) and community respiration (the utilization of that organic carbon by both autotrophs and heterotrophs) indicates whether organic material is locally in excess or demand (12, 13). Net ecosystem production (NEP, also referred to as net ecosystem metabolism or net community production in oceanography) is therefore a quantification of how neighboring ecosystems interact: An ecosystem that is net autotrophic ($NEP > 0$) has organic material available for local burial and/or export to adjacent ecosystems; conversely, a net heterotrophic ecosystem ($NEP < 0$) requires stored or imported organic matter to maintain its metabolic state (7, 14). There have been numerous studies seeking to explain patterns in aquatic ecosystem metabolism (15–22), but a unifying framework of these diverse ecosystems has proved elusive.

The purpose of this paper is to show that estuarine ecosystem metabolism varies predictably with size. Such patterns have been noted previously in both estuarine and lacustrine systems (17, 23), but the fundamental origin of this organization has not been explored. The significance of this study is not simply that larger estuaries have lower specific (on a per unit size basis) ecosystem metabolism than smaller estuaries, but that this size scaling arises because the residence time of limiting nutrients does not scale isometrically with size.

The motivation for this synthesis is rooted in recent discussions in evolutionary biology (21, 24–26), where it has long been noted that many organismal metabolic processes b_i scale with body size v_i to the 3/4 power: $b_i \sim v_i^{3/4}$ (27); the subscript i denotes an individual or organismal term. (On a log-log plot, the nonlinear relationship between b_i and v_i is linear with slope $\alpha = 3/4$, as $\log b_i = \log v_i^{\alpha} = \alpha \log v_i$. The scaling exponent $\alpha = 1$ for a linear, isometric relationship and $\alpha \neq 1$ for a nonlinear, allometric relationship.) This empirical relationship has been explained theoretically as arising from limitations of transport: Because blood velocities vary by only 1 order of magnitude in

Significance

Coastal margins host some of the most productive habitats on the planet, yet there is still significant uncertainty about the magnitude of carbon fluxes across the land/ocean interface. Scaling up in situ measurements into whole-ecosystem estimates of how these habitats contribute to global biogeochemical cycling has been hindered by their apparent heterogeneity, complex circulation, and sizes that range from tens of meters to hundreds of kilometers. Here, I show that estuarine ecosystem metabolism varies predictably with ecosystem size. The significance of this study is not simply that larger estuaries have lower specific ecosystem metabolism than smaller estuaries, but that this size scaling arises because the residence time of limiting nutrients does not scale isometrically with estuary size.

Author contributions: N.J.N. designed research, performed research, analyzed data, and wrote the paper.

The author declares no conflict of interest.

This article is a PNAS Direct Submission.

[1]Email: nidzieko@ucsb.edu.

This article contains supporting information online at www.pnas.org/lookup/suppl/doi:10.1073/pnas.1719963115/-/DCSupplemental.

Published online June 11, 2018.

animals that span 12 orders of magnitude in size, the capacity to transport metabolites throughout a circulatory system does not increase isometrically with organismal size and so larger animals must have lower specific metabolic rates than smaller animals (24, 28, 29). In estuaries that span more than 10 orders of magnitude in size, the magnitude of tidal, wind-driven, and density-driven currents varies by roughly an order of magnitude, and so—analogous to organismal metabolism—it stands to reason that larger ecosystems must support less primary production on a per unit size basis than smaller ecosystems because the transport of limiting nutrients scales allometrically (nonlinearly with size).

To test the hypothesis that ecosystem metabolism varies predictably with system size, I compiled published gross primary production ($n = 134$) and community respiration ($n = 88$) data for coastal ecosystems. The majority of the data points are derived from estuaries where metabolic rates were determined through open-water and/or budget methods (9) and are presented as published. Estimates of estuary size were obtained from the primary reporting source (where available), other publications, or measurements of aerial images (*SI Appendix*, Table S1). The slopes (scaling exponents) reported are the result of ordinary least-squares regression preformed on $\log_{10}$-transformed data, presented with 95% confidence intervals. Further details of the statistical treatment of the dataset, including the choice of regression, are contained in *SI Appendix* (*SI Appendix*, Fig. S3). Although these system-level rates are most specifically labeled coastal aquatic community metabolism because these methods generally omit the metabolism of emergent vegetation (e.g., tidal marshes) when those plants are not inundated, I use the phrase ecosystem metabolism for narrative purposes. The geomorphologic scope of the dataset spans from the limit of salt intrusion to the inner shelf, including bays, fjords, coastal seas, and tropical mangrove lagoons. With apologies to Pritchard (30), I refer collectively to all of these as estuaries for the similar biogeochemical role that they play at the land–sea interface.

When using the full dataset, gross primary production P, in units of grams C·d^{-1}, scales with the fluid volume V as $P \sim V^{0.75}$ (Table 1 and Fig. 1). The scaling exponent α for gross primary production as a function of wetted surface area A (generally the area flooded at mean high water) is statistically less than one ($P \sim A^{0.91}$) at the 95% confidence interval. There is a nonisometric relationship between mean depth H and area in these ecosystems ($H \sim A^{0.16}$, Fig. 1*B*). Community respiration R scales with volume to the 0.77 power and area to the 0.90 power, results that are not statistically different from the scaling of primary production as a function of size (Table 1 and *SI Appendix*, Fig. S1). Statistically equivalent slopes are obtained for specific metabolism as a function of size (e.g., $P/A \sim A^{1-\alpha}$; *SI Appendix*, Fig. S3), removing the possibility that the regression results are due to size factoring into total metabolism.

These results are notable on two points. First, it is intriguing that ecosystem metabolism scales with volume similar to the scaling between organismal metabolism and size. And second, these results show that P does not scale linearly with surface area, as might be expected given the importance of solar irradiance to primary production.

In the remainder of this paper, I apply theoretical arguments developed for organismal metabolic scaling to pose an explanation for how and why this size scaling is manifest in estuaries. I refer generically to ecosystem metabolism, B, in developing the theoretical arguments.

Metabolic Scaling for Estuaries

Consider an estuary of areal extent A and mean depth H with volume $V = AH$. Within this ecosystem there are n organisms that produce or respire organic carbon with an abundance per unit volume (organismal density) $\Gamma = n/V$. Primary production and the formation of new biomass is generally limited by the availability of fixed inorganic nitrogen (31); respiration of organic carbon is tightly coupled to this production (Table 1 and *SI Appendix*, Fig. S1). Conservation of mass requires ecosystem metabolism to be the sum of the individual metabolic rates or, equivalently, the average (denoted by the overbar) organismal rate times the number of individuals: $B = \sum_n b_i = n\bar{b}_i$ (32). Total ecosystem metabolism

$$B = V\Gamma\bar{b}_i = VE \qquad [1]$$

is therefore a function of ecosystem size V and the average metabolic rate per unit volume, $B/V = E = \Gamma\bar{b}_i$. To explain the observations in Fig. 1, the goal is to establish how B and E vary with the size of the ecosystem V.

Table 1. Regression results and statistics in Figs. 1 and 3

	All		Shallow		Deep	
Scaling relationship	β	α	β	α	β	α
Fig. 1						
$P \sim \beta A^{\alpha}$	0.64	0.91	0.49	0.94	0.55	0.91
	(0.36:0.91)	(0.87:0.94)	(0.10:0.88)	(0.88:1.00)	(0.04:1.05)	(0.85:0.97)
	SE = 0.36, n = 134		SE = 0.38, n = 63		SE = 0.34, n = 71	
$P \sim \beta V^{\alpha}$	1.43	0.75	0.65	0.90	1.32	0.75
	(1.08:1.77)	(0.71:0.79)	(0.23:1.07)	(0.83:0.96)	(0.65:1.98)	(0.67:0.82)
	SE = 0.50, n = 134		SE = 0.42, n = 63		SE = 0.48, n = 71	
$H \sim \beta A^{\alpha}$	−0.67	0.16	−0.10	0.04	−0.34	0.14
	(−0.95:-0.39)	(0.12:0.20)	(−0.27:0.06)	(0.01:0.06)	(−0.89:0.20)	(0.07:0.21)
	SE = 0.37, n = 134		SE = 0.16, n = 63		SE = 0.37, n = 71	
Fig. 3						
$P/R \sim \beta A^{\alpha}$	−0.19	0.013	−0.08	−0.006	−0.29	0.028
	(−0.33:−0.04)	(−0.007:0.033)	(−0.24:0.08)	(−0.031:0.019)	(−0.62:0.05)	(−0.013:0.070)
	SE = 0.17, n = 88		SE = 0.15, n = 51		SE = 0.19, n = 37	
$P/R \sim \beta V^{\alpha}$	−0.18	0.012	−0.07	−0.007	−0.26	0.023
	(−0.32:−0.05)	(−0.006:0.029)	(−0.24:0.09)	(−0.031:0.018)	(−0.59:0.07)	(−0.014:0.060)
	SE = 0.17, n = 88		SE = 0.15, n = 51		SE = 0.19, n = 37	

For each regression, the first line is the coefficient (β) and scaling exponent (α). The second line, in parentheses, is the 95% confidence interval range. The third line provides the SE of the regression and the number of data points.

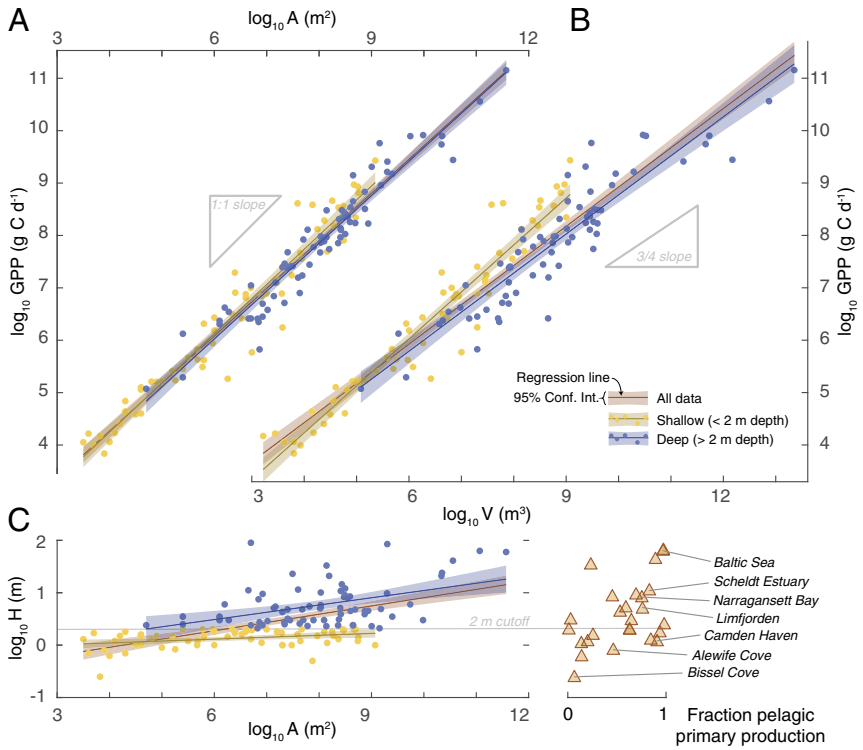

Fig. 1. (*A* and *B*) Gross primary production as a function of (*A*) surface area and (*B*) volume. (*C*) Depth as a function of area. Regression lines in *A*–*C* are for the full dataset (orange), systems shallower than 2 m (yellow), and systems deeper than 2 m (blue). Shading indicates 95% confidence interval. Systems listed in *C*, *Right* show relative fraction of pelagic gross primary production as a function of depth. Statistics are shown in Table 1. Plots and regressions for community respiration and specific metabolism are in *SI Appendix*, Figs. S1 and S2 and Table S2.

One possibility is to suppose that E is independent of V. Indeed, this is the result that is obtained if well-documented allometric relationships for abundance and metabolism as a function of organismal size are applied to **Eq. 1** (32). As organismal size v_i increases, metabolic rate increases (33) $\bar{b}_i \sim v_i^{\alpha}$ while abundance decreases (34, 35) $\Gamma \sim v_i^{-\alpha}$. The scaling exponent α for the size–metabolism relationship in marine phytoplankton is often observed to be close to Kleiber's 3/4 scaling (27), with deviations due to the physiology of nutrient uptake limitation (33); abundance is generally found to scale as the reciprocal of metabolism (36, 37). Inserting these relationships into **Eq. 1** yields the prediction that ecosystem metabolism is independent of organism size and so scales linearly with ecosystem size: $B \sim V v_i^{-\alpha} v_i^{\alpha} = V v_i^0$; equivalently, the specific metabolic rate is independent of ecosystem size: $B/V = E \sim V^0$. In contrast, the observations show that specific metabolism scales as $E \sim V^{-1/4}$ and I argue next that this is because nutrient residence time does not scale isometrically with ecosystem size.

The relationships in Eq. **1** and observations in Fig. 1 can be explained by modeling the nutrient delivery that supports coastal ecosystem metabolism as an efficient, directed-transport network (24, 26, 38), the scaling of which predicts how metabolic demand is limited by the flux of material through the system as a function of its size and dimensionality. For a D-dimensional system, it has been shown theoretically (24, 38) that efficient material flux (which is equal to the metabolic demand B at steady state) scales allometrically with the size of the transport network Q as

$$B \sim Q^{\frac{D}{(D+1)}}. \qquad [2]$$

How metabolic demand ultimately scales with the system size depends on whether the transport network (i.e., the fluid environment) is internal or external to the system. This is evident in two cases: (*i*) pelagic ecosystems, where the transport network is internal to the system (and, in fact, is the system) and organisms are distributed in 3D space, and (*ii*) benthic ecosystems, where the transport network is external to the system and organisms are distributed in 2D space. In the case of pelagic ecosystems, the volume of the transport network is constrained to scale isometrically with system size: $Q \approx V \approx L^D$, where L is a characteristic physical length scale and $D = 3$. Combining this constraint with Eq. **2**, $B \sim \left(L^D\right)^{\frac{D}{D+1}} \approx V^{3/4}$ predicts that pelagic ecosystem metabolism should scale with volume to the 3/4 power (equivalently, specific ecosystem metabolism should scale with size to the $-1/4$ power: $B/V = E \sim V^{-1/4}$). In the case of benthic ecosystems, size is defined by area $A \sim L^D$ with $D = 2$; the fluid transport is external to the benthos, however, and so the transport network contains an extra dimension than the arrangement of metabolic sites (i.e., organisms): $Q \sim L^{D+1}$. Combining this with Eq. **2**, $B \sim \left(L^{D+1}\right)^{\frac{D}{D+1}} \sim L^D \sim A$ predicts that benthic ecosystem metabolism should scale linearly with area (equivalently, specific metabolism should be independent of area: $E \sim A^0$).

This theoretical scaling suggests there are two limits for estuarine ecosystem metabolism: shallow and deep. Primary production should shift from scaling linearly with area across shallow systems dominated by benthic primary production to scaling with volume to the 3/4 power across deeper ecosystems dominated by pelagic primary production.

The two scaling limits for benthic and pelagic ecosystems become evident when the dataset is separated into shallow and deep subsets. Here I use a depth threshold of 2 m, which is consistent with a shift from predominantly benthic to pelagic primary production (Fig. 1*C*); the results are not overly sensitive to this cutoff (discussion in *SI Appendix*). There is good agreement

between the observations and predicted scaling, particularly given that the compiled results have not been adjusted for nutrient loading, temperature, latitude, habitat, or methodological differences (39). Across shallow ecosystems, $P \sim A^{0.94} \sim V^{0.90}$ and $H \sim A^{0.04}$; metabolism across the deep ecosystems scales as $P \sim V^{0.75} \sim A^{0.91}$ and $H \sim A^{0.14}$ (Table 1 and Fig. 1). The scaling for metabolism as a function of area in the deep subset is statistically different from $P \sim A$ at the 95% confidence interval.

Residence Time

One conclusion to be drawn from these results is that a 3D transport network is a fundamental aspect of estuarine ecosystem metabolism. This is notable insofar as a typical approach in estuarine physics is to simplify the equations of motion on the basis of geometric scales. Typically, estuaries are much longer than they are wide and many orders of magnitude longer than they are deep ($L_x >> L_y >> L_z$); these order of magnitude differences in geometry allow the Navier–Stokes equations to be reduced to the leading-order terms at the scale of interest, such as the along-channel response of estuarine salinity structure to river flow and tidal mixing (40). Given this typical hydrodynamics approach, it might be expected that ecosystem metabolism would also scale as a one-dimensional network. But a one-dimensional ecosystem is inconsistent with the observation that $B \sim V^{3/4}$, because $B \sim Q^{1/2}$ (from Eq. **2** with $D = 1$) would require a transport network that increased superlinearly with size: $Q \sim V^{3/2}$. For a 2D transport network, Eq. **2** predicts $B \sim Q^{2/3}$; under the constraints of fluid transport ($Q \sim V$), pelagic metabolism would scale as $B \sim V^{2/3}$, a result that is statistically unlikely given the error bounds in Table 1. Therefore, the only scenario that can match both the observations and scaling arguments across benthic and pelagic ecosystems is one where nutrient delivery to primary producers within aquatic ecosystems occurs through a transport network that scales three-dimensionally as $Q \sim L^3$, a result that is central to understanding the observations.

We can understand the different scaling in benthic and pelagic marine ecosystems by considering the relevant timescales. Banavar et al. (26, 38) define a service volume ℓ^D that satisfies the constraint $E\ell^D \sim V^0$. By definition, the volume (for $D = 3$) or area (for $D = 2$) ℓ^D is inversely proportional to the specific metabolic rate and so ℓ scales the distance traveled by a metabolite in a unit of time τ given the speed u at which that metabolite is transported through the ecosystem: $\ell = u\tau$. The metabolic time is the reciprocal of a characteristic organismal growth rate $\tau = \mu^{-1}$ and is independent of ecosystem size (41, 42).

Introducing $E \sim \ell^{-D}$ into Eq. **1**, we can rearrange the terms to understand that patterns in ecosystem metabolism as a function of ecosystem size are driven by changes in the ratio of a transport time to growth time,

$$B \sim \left(\frac{L}{\ell}\right)^D \approx \left(\frac{L\mu}{u}\right)^D \approx \left(\frac{T}{\tau}\right)^D, \qquad [3]$$

where $T = L/u$ is a system-scale transport time: the average residence time of new, nutrient-rich water entering the system. The same ratio of parameters $L\mu/u$ emerges independently from dimensional analysis, lending support to efficient transport network scaling (*SI Appendix*). Eq. **3** shows that as residence time increases, total metabolism also increases; as the growth rate goes to zero, metabolic time becomes infinite and total metabolism goes to zero.

Combining Eqs. **2** and **3** produces a relation for residence time as a function of the size and dimensionality of the transport network: $T \sim Q^{1/(D+1)}$ (24). I have shown that the size of the transport network in both benthic and pelagic ecosystems scales as $Q \sim L^3$, and so we have the insight that nutrient residence time in estuaries scales isometrically with size $T \sim L$ across shallow systems but allometrically with size $T \sim L^{3/4}$ across deep systems. Equivalently, the characteristic velocity scales as $u \sim L^0$ across shallow systems and $u \sim L^{1/4}$ across deep systems.

Although this velocity scaling emerges from consideration of the spatial and temporal scales of material flux through a generic transport network, it is consistent with the fact that velocity is a function of depth in estuaries. For example, the freshwater Froude number $\mathrm{Fr}_f = u/(\beta g S_{\mathrm{ocean}} H)^{1/2}$ (the net velocity due to river flow scaled by the maximum possible frontal propagation speed, where $\beta g S_{\mathrm{ocean}}$ approximates the along-estuary baroclinic density gradient with a coefficient of haline contraction, gravity, and the ocean salinity) must be less than or equal to one, and so u scales at most as $H^{1/2}$ for baroclinic flows; likewise, the barotropic tide is balanced by a friction term where $u \sim H^{1/2}$. Therefore, it naturally follows that velocity is constant (in a scaling sense) across shallow systems because the depth is constant ($H \sim A^0$), whereas velocity increases allometrically with pelagic ecosystem size owing to the allometric geometry.

It is perhaps counterintuitive that increasing velocity leads to sublinear size scaling for pelagic ecosystem metabolism, given the general paradigm that production is intrinsically linked to mechanical energy (43, 44). One might reason that an increasing velocity with increasing ecosystem size would lead to greater productivity per unit area, but the metabolic time remains fixed and so increasing velocity results in a larger service volume, with the consequence that metabolism per unit size decreases (Fig. 2).

Finally, we consider how net ecosystem production scales with size. While $NEP = P - R$, P/R is plotted for representation on a log scale, such that $\log_{10} P/R < 0$ is net heterotrophic. Both the regression of P/R as a function of size (Fig. 3) and the ratio of the coefficients derived individually for P and R (Table 1) indicate that most estuaries are net heterotrophic, consistent with the current consensus from budget estimates (3, 20). This synthesis shows that NEP is a positive function of both area

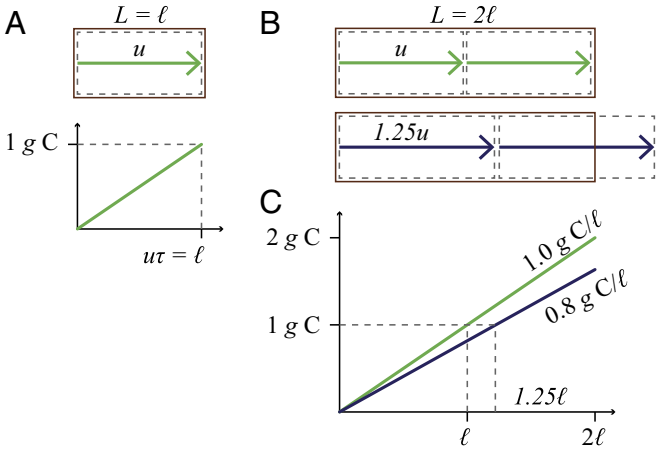

Fig. 2. Consider an ecosystem (*A*) of size $L = \ell$, where $\ell = u\tau$, τ is an ecosystem-independent growth time, and u is a transport velocity carrying nutrients to and through the ecosystem. The graph depicts the accumulation of organic carbon along the flow path for an ecosystem metabolism of 1 g C per unit time or, equivalently, 1 g C per ℓ. This corresponds to the service volume, shown in dashed lines. Ecosystems *B* and *C* are both twice as long as *A*, but the velocity in *C* is 1.25 times larger than the velocity in either *A* or *B*. The increased velocity in *C* results in a lower specific metabolism than in *B* because the residence time is shorter.

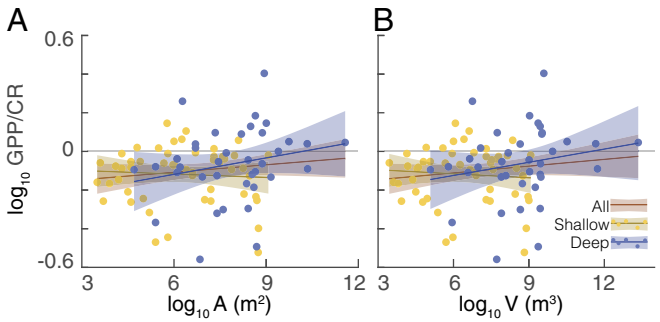

Fig. 3. NEP as a function of surface area. Regression lines in *A* and *B* are for the full dataset (orange), systems shallower than 2 m (yellow), and those deeper than 2 m (blue). Shading indicates 95% confidence interval. Statistics are shown in Table 1.

and volume, indicating a shift toward net autotrophy in larger, deeper ecosystems, although the error bounds are large. While clearly numerous factors contribute to the metabolic poise of an ecosystem (39, 45), this shift is reasonable in the context of the residence time dynamics discussed above. If we consider that there is a time lag between the formation of new organic carbon via net primary production and the respiration of that organic matter by grazers and/or decomposers and that this time lag is independent of ecosystem size, then the fraction of locally produced organic matter that is also locally respired within the system must decrease as velocities increase. With isometric transport across shallow systems, larger systems are just as efficient at retaining material as smaller systems and so show no change in NEP.

Summary and Applications

I compiled gross primary production, community respiration, and geomorphological data to test the hypothesis that estuarine ecosystem metabolism varies predictably with size. I found that that size-dependent patterns in gross primary production and community respiration exist across a wide range of coastal geomorphologies. Scaling arguments for transport networks derived to explain patterns in organismal biology, as well as dimensional analysis, provide a plausible explanation for the observation that deeper systems, which are dominated by pelagic primary production, scale with volume to the 3/4 power whereas metabolic rates across shallow systems scale nearly linearly with area and volume. The main conclusion from this synthesis is that the residence time of new, nutrient-rich water is the basic organizing principle for the observed patterns of ecosystem metabolism. Residence time changes allometrically with size in pelagic ecosystems because velocities change by an order of magnitude across systems that span more than 10 orders of magnitude in size; a nonisometric change in velocity with size requires lower specific metabolic rates at larger ecosystem sizes.

These results may provide a unifying framework for the synthesis of coastal processes on regional and global levels. One such application could be to use the scaling equations to represent biogeochemical processes at subgrid scales in global geochemical models, although further work to reduce the error bounds is required to this end. Another possible application is the formulation of detailed carbon-cycling budgets using very basic data that can be derived from aerial imagery. For example, the empirical coefficients for the shallow and deep systems (as a function of area) can be applied to the estuarine intertidal (E1) and subtidal (E2) habitat types, respectively, in the US National Fish and Wildlife National Wetland Inventory dataset (46) (Table 2). Taken in sum, this method provides regional

Table 2. Estuarine ecosystem metabolism estimates for marine coastlines of the continental United States using values in Table 1

	Pacific	Gulf of Mexico	Atlantic
GPP, Tg C·y^{-1}	**0.4 (0.2, 0.9)**	**3.1 (2.5, 3.9)**	**3.2 (2.3, 4.6)**
Intertidal	0.3 (0.1, 0.8)	1.4 (0.9, 2.2)	2.0 (1.2, 3.5)
Subtidal	0.1 (0.1, 0.2)	1.7 (1.5, 2.0)	1.2 (1.0, 1.3)
CR, Tg C·y^{-1}	**0.6 (0.3, 1.3)**	**3.8 (2.8, 5.1)**	**4.6 (2.9, 7.2)**
Intertidal	0.5 (0.2, 1.3)	2.2 (1.4, 3.6)	3.4 (1.9, 6.1)
Subtidal	0.1 (0.1, 0.2)	1.5 (1.4, 1.7)	1.1 (1.0, 1.2)
NEP, Tg C·y^{-1}	**−0.2 (−1.4, 1.0)**	**−0.7 (−3.4, 2.0)**	**−1.4 (−6.2, 3.5)**
Intertidal	−0.2 (−1.4, 1.1)	−0.8 (−3.4, 1.7)	−1.4 (−6.2, 3.5)
Subtidal	−0.0 (−0.0, 0.0)	0.2 (−0.5, 0.8)	0.0 (−0.3, 0.4)
Total area, km^2	**6,220**	**46,349**	**45,950**
Intertidal	4,270	17,228	28,705
Subtidal	1,950	29,121	17,245

Intertidal and subtidal areas are derived from the United States Fish and Wildlife Service National Wetlands Inventory (USFW NWI) dataset habitats E1 and E2, respectively (46). GPP and CR are estimated using shallow and deep regression results (Table 1) applied to the polygon-level delineations of E1 and E2, respectively, and then summed (shown in bold). NEP was calculated by difference of these values. Confidence limits, in parentheses, represent 95% bounds determined by Monte Carlo estimation of 1,000 realizations that include the SE of the regressions. Polygons smaller than 10 m^2 are not included.

estimates of the role of estuaries in carbon cycling. Using this method, I estimate that estuaries along the US Atlantic Coast support 3.2 Tg C·y^{-1} of gross primary production and respire 4.6 Tg C·y^{-1}, with a net balance of −1.4 Tg C·y^{-1} over a total estuarine area of 45,950 km^2, or −2.5 mol C·m^{-2}·y^{-1} (Table 2). Herrmann et al. (20) estimate via a detailed budget synthesis using the National Estuarine Eutrophication Assessment survey (47) that NEP for US East Coast estuaries is −1.5 Tg C·y^{-1} over an area of 37,764 km^2, equivalent to −3.3 mol C·m^{-2}·y^{-1}. With an improved understanding of why and how individual ecosystems deviate from the broader size-scaling trend, allometric scaling may be used to create robust estimates of the contribution that estuaries make to the global carbon cycle.

Summary of terms

α	The scaling exponent in a power-law relationship, $y = \beta x^{\alpha}$
β	Coefficient in power-law relationship
H	Average depth
A	Wetted surface area
V	Volume of the estuary, $V = AH$
P	Gross primary production (GPP)
R	Community respiration (CR)
B	A measure of ecosystem metabolism, i.e., either GPP or CR
NEP	Net ecosystem production, $NEP = P - R$
E	Specific metabolic rate, $E = B/V$
Q	Size of the transport network carrying metabolites
D	Effective dimensionality of the system, i.e., number of dimensions required to describe the distribution of metabolic sites
L	Characteristic physical length scale of an estuary
u	Characteristic transport velocity through the estuary
μ	Organismal growth rate
τ	Timescale associated with organismal metabolism, $\tau = \mu^{-1}$
ℓ	Length scale set by transport velocity and metabolic time, $\ell = u\tau$
T	Transport timescale in the estuary, $T = L/u$

ACKNOWLEDGMENTS. R. Saba and D. M. Ferraro helped with primary source data retrieval. I am grateful for discussions with A. E. Santoro, J. J. Pierson, W. Z. Haskell, and J. M. Testa at various stages of this research, as well as the constructive comments of three anonymous reviewers. Support was provided by National Science Foundation Awards OCE-1259691 and OCE-1334398.

1. Gattuso JP, Frankignoulle M, Wollast R (1998) Carbon and carbonate metabolism in coastal aquatic ecosystems. *Annu Rev Ecol Syst* 29:405–434.
2. Cebrian J (2002) Variability and control of carbon consumption, export, and accumulation in marine communities. *Limnol Oceanogr* 47:11–22.
3. Bauer JE, et al. (2013) The changing carbon cycle of the coastal ocean. *Nature* 504: 61–70.
4. Borges AV (2005) Do we have enough pieces of the jigsaw to integrate CO2 fluxes in the coastal ocean? *Estuaries* 28:3–27.
5. Bouillon S, et al. (2008) Mangrove production and carbon sinks: A revision of global budget estimates. *Global Biogeochem Cycles* 22:GB2013.
6. Dai M, Yin Z, Meng F, Liu Q, Cai WJ (2012) Spatial distribution of riverine DOC inputs to the ocean: An updated global synthesis. *Curr Opin Environ Sustainability* 4:170–178.
7. Cai WJ (2011) Estuarine and coastal ocean carbon paradox: CO2 sinks or sites of terrestrial carbon incineration? *Annu Rev Mar Sci* 3:123–145.
8. Barbier EB, et al. (2011) The value of estuarine and coastal ecosystem services. *Ecol Monogr* 81:169–193.
9. Staehr P, et al. (2012) The metabolism of aquatic ecosystems: History, applications, and future challenges. *Aquat Sci* 74:1–15.
10. Odum HT (1956) Primary production in flowing waters. *Limnol Oceanogr* 1:102–117.
11. Odum HT, Hoskin CM (1958) Comparative studies on the metabolism of marine waters. *Contrib Mar Sci* 5:16–46.
12. Testa J, Kemp W (2008) Variability of biogeochemical processes and physical transport in a partially stratified estuary: A box-modeling analysis. *Mar Ecol Prog Ser* 356: 63–79.
13. Ahlström A, et al. (2015) The dominant role of semi-arid ecosystems in the trend and variability of the land CO2 sink. *Science* 348:895–899.
14. Kemp WM, Smith EM, Marvin-DiPasquale M, Boynton WR (1997) Organic carbon balance and net ecosystem metabolism in Chesapeake Bay. *Mar Ecol Prog Ser* 150:229–248.
15. Nixon S, et al. (1996) The fate of nitrogen and phosphorus at the land-sea margin of the North Atlantic Ocean. *Biogeochemistry* 35:141–180.
16. Caffrey J (2004) Factors controlling net ecosystem metabolism in US estuaries. *Estuaries Coasts* 27:90–101.
17. Hood WG (2007) Landscape allometry and prediction in estuarine ecology: Linking landform scaling to ecological patterns and processes. *Estuaries Coast* 30: 895–900.
18. Hoellein TJ, Bruesewitz DA, Richardson DC (2013) Revisiting Odum (1956): A synthesis of aquatic ecosystem metabolism. *Limnol Oceanogr* 58:2089–2100.
19. Huete-Ortega M, et al. (2014) Distinct patterns in the size-scaling of abundance and metabolism in coastal and open-ocean phytoplankton communities. *Mar Ecol Prog Ser* 515:61–71.
20. Herrmann M, et al. (2015) Net ecosystem production and organic carbon balance of US East Coast estuaries: A synthesis approach. *Glob Biogeochem Cycles* 29:96–111.
21. Schramski JR, Dell AI, Grady JM, Sibly RM, Brown JH (2015) Metabolic theory predicts whole-ecosystem properties. *Proc Natl Acad Sci USA* 112:2617–2622.
22. Acevedo-Trejos E, Brandt G, Bruggeman J, Merico A (2015) Mechanisms shaping size structure and functional diversity of phytoplankton communities in the ocean. *Sci Rep* 5:8918.
23. Glazier DS (2014) Metabolic scaling in complex living systems. *Systems* 2:451–540.
24. Banavar JR, Maritan A, Rinaldo A (1999) Size and form in efficient transportation networks. *Nature* 399:130–132.
25. Dodds PS, Rothman DH, Weitz JS (2001) Re-examination of the "3/4-law" of metabolism. *J Theor Biol* 209:9–27.
26. Banavar JR, et al. (2010) A general basis for quarter-power scaling in animals. *Proc Natl Acad Sci USA* 107:15816–15820.
27. Kleiber M (1932) Body size and metabolism. *Hilgardia* 6:315–353.
28. West GB, Brown JH, Enquist BJ (1997) A general model for the origin of allometric scaling laws in biology. *Science* 276:122–126.
29. West GB, Brown JH, Enquist BJ (1999) The fourth dimension of life: Fractal geometry and allometric scaling of organisms. *Science* 284:1677–1679.
30. Pritchard DW (1952) Estuarine hydrography. *Adv Geophys* 1:243–280.
31. Falkowski PG, Barber RT, Smetacek V (1998) Biogeochemical controls and feedbacks on ocean primary production. *Science* 281:200–206.
32. Enquist BJ, et al. (2003) Scaling metabolism from organisms to ecosystems. *Nature* 423:639–642.
33. Irwin AJ, Finkel ZV, Schofield OM, Falkowski PG (2006) Scaling-up from nutrient physiology to the size-structure of phytoplankton communities. *J Plankton Res* 28:459–471.
34. Cermeno P, et al. (2008) Resource levels, allometric scaling of population abundance, and marine phytoplankton diversity. *Limnol Oceanogr* 53:312–318.
35. Beardall J, et al. (2009) Allometry and stoichiometry of unicellular, colonial and multicellular phytoplankton. *New Phytol* 181:295–309.
36. Damuth J (1981) Population density and body size in mammals. *Nature* 290:699–700.
37. Huete-Ortega M, Cermeño P, Calvo-Díaz A, Marañón E (2012) Isometric size-scaling of metabolic rate and the size abundance distribution of phytoplankton. *Proc R Soc B* 279:1815–1823.
38. Banavar JR, Damuth J, Maritan A, Rinaldo A (2002) Supply–demand balance and metabolic scaling. *Proc Natl Acad Sci USA* 99:10506–10509.
39. Harris LA, Duarte CM, Nixon SW (2006) Allometric laws and prediction in estuarine and coastal ecology. *Estuaries Coast* 29:340–344.
40. Geyer WR, MacCready P (2014) The estuarine circulation. *Annu Rev Fluid Mech* 46:175–197.
41. Eppley RW (1972) Temperature and phytoplankton growth in the sea. *Fish Bull* 70:1063–1085.
42. Cael B, Follows MJ (2016) On the temperature dependence of oceanic export efficiency. *Geophys Res Lett* 43:5170–5175.
43. Margalef R (1978) Life-forms of phytoplankton as survival alternatives in an unstable environment. *Oceanol Acta* 1:493–509.
44. Nixon SW (1988) Physical energy inputs and the comparative ecology of lake and marine ecosystems. *Limnol Oceanogr* 33:1005–1025.
45. Dodds WK, Cole JJ (2007) Expanding the concept of trophic state in aquatic ecosystems: It's not just the autotrophs. *Aquat Sci* 69:427–439.
46. US Fish and Wildlife Service (2017) *National Wetlands Inventory* (US Department of the Interior, Fish and Wildlife Service, Washington, DC). Available at https://www.fws.gov/wetlands/. Accessed May 1, 2017.
47. Bricker S, et al. (2007) *Effects of Nutrient Enrichment in the Nation's Estuaries: A decade of Change*, *National Estuarine Eutrophication Assessment Update*, NOAA Coastal Ocean Program Decision Analysis Series No. 26 (National Centers for Coastal Ocean Science, Silver Spring, MD).